© 2015. Published by The Company of Biologists Ltd | Journal of Cell Science (2015) 128, 4126-4137 doi:10.1242/jcs.174664

RESEARCH ARTICLE

Rabaptin5 is recruited to endosomes by Rab4 and Rabex5 to regulate endosome maturation

Simone Kälin, David T. Hirschmann, Dominik P. Buser and Martin Spiess*

ABSTRACT

Rab GTPases control membrane identity, fusion and transport by interaction with effector proteins. Effectors that influence the activation–inactivation cycle of their own or other Rab proteins contribute to the timely conversion of Rab membrane identities. Rab5 and its effector rabaptin5 (Rbpt5, also known as RABEP1) are generally considered the prime example for a positive-feedback loop in which Rab5-GTP recruits Rbpt5 in complex with Rabex5 (also known as RABGEF1), the GDP/GTP exchange factor of Rab5, to early endosomes, thus maintaining the Rab5 membrane identity. By deletion analysis, we found that the membrane recruitment of Rabaptin5 required binding to Rab4 and Rabex5, but not Rab5. Deletion of either one of the two Rab5-binding domains or silencing of Rab5 expression did not affect Rabaptin5 recruitment, but produced giant endosomes with early and late endosomal characteristics. The results contradict the model of feedback activation of Rab5 and instead indicate that Rbpt5 is recruited by both Rabex5 recognizing ubiquitylated cargo and by Rab4 to activate Rab5 in a feed-forward manner.

KEY WORDS: Rabaptin5, Rabex5, Rab GTPase

INTRODUCTION

Membrane traffic and organelle morphology are regulated by Rab proteins, small GTPases that exist in active GTP-bound and inactive GDP-bound forms (Barr, 2013; Mizuno-Yamasaki et al., 2012; Pfeffer, 2013; Stenmark, 2009). They are activated by guanine nucleotide exchange factors (GEFs) at the target membrane (Blümer et al., 2013) and inactivate themselves by their intrinsic GTPase activity that is further stimulated by GTPase-activating proteins (GAPs). In their active state, Rab proteins bind to effectors to mediate their functions, such as protein sorting, organelle motility, membrane tethering or lipid modification. Networks of interacting proteins are formed that change with time in their properties and composition. Various modes of Rab coordination have been proposed (Stenmark, 2009): (1) positive feedback, where a Rab recruits its own GEF, thus maintaining the Rab identity of the membrane; (2) effector coupling, where the effector of one Rab also interacts with another and thereby coordinates or couples different Rab domains or Rab activities in the same membrane; (3) activation coupling, where one Rab recruits the GEF of a second Rab in a feed-forward manner; and finally, (4) Rab conversion, where the first Rab recruits the GEF of the second which then recruits a GAP for the first, thereby completing the full transition from one Rab identity of the membrane to the next. Rabaptin5 (Rbpt5, also known as RABEP1) is generally considered the prime example of a Rab effector mediating a positive-feedback loop (mechanism 1) to maintain high Rab5 activity on early endosomes, and effector coupling (mechanism 2) to connect Rab5 to Rab4 (Fig. 1A) (Barr, 2013; De Renzis et al., 2002; Horiuchi et al., 1997; Mizuno-Yamasaki et al., 2012; Stenmark, 2009; Zerial and McBride, 2001). Note, that Rab4 has two isoforms (a and b) and Rab5 has three isoforms (a, b and c).

Rbpt5 is a cytosolic protein recruited to early transferrin (Tf)-positive endosomes where it acts as a regulator of endosome morphology and function. It is an 862-residue protein containing heptad-repeat sequences that form coiled-coil dimers (illustrated in Fig. 1B, top). It was initially isolated as an interactor of Rab5 (Stenmark et al., 1995). It specifically binds Rab5-GTP through a C-terminal domain (residues 814–862; Vitale et al., 1998; Zhu et al., 2004b), but yeast two-hybrid and glutathione-S-transferase (GST)–Rab5 pulldown experiments have also observed some interaction through a second site in the N-terminal part of the protein (Deneka et al., 2003; Vitale et al., 1998), specifically in the segment 216–318 (Korobko et al., 2006). In addition, Rbpt5 associates, through its CC2-1 coiled-coil segment, to Rabex5 (also known as RABGEF1), the GEF of Rab5 (Horiuchi et al., 1997; Mattera et al., 2006). Most of Rabex5 in the cytosol has been found in a 2:1 Rbpt5–Rabex5 complex (Lippé et al., 2001).

Rab5 controls early endosome fusion by binding to several additional effector proteins (Kümmel and Ungermann, 2014; Ohya et al., 2009). It activates phosphatidylinositol 3-kinases (PI3Ks), particularly Vps34 (also known as PIK3C3) and p150 (also known as PIK3R4) to generate phosphatidylinositol 3-phosphate (PI3P), the hallmark lipid of early endosomes (Christoforidis et al., 1999b). It further binds to early endosome antigen 1 (EEA1) and rabenosyn-5, two multivalent proteins containing FYVE domains that bind to PI3P, and that are able to bridge two membranes as tethers (Christoforidis et al., 1999a; Nielsen et al., 2000). Rabenosyn-5 forms a complex with Vps45, an SM (Sec1–Munc18) family protein stimulating SNARE assembly and membrane fusion (Nielsen et al., 2000).

Activation of Rab5 by overexpression of wild-type or constitutively active Rab5 therefore produces enlarged endosomes as a result of increased early endosome fusion (Bucci et al., 1992; Stenmark et al., 1994). The same was observed upon overexpression of the GEF Rabex5 (Mattera and Bonifacino, 2008) or of Rbpt5 (Stenmark et al., 1995). In an *in vitro* assay, the Rbpt5–Rabex5 complex was found to be much more potent in stimulating Rab5-mediated membrane fusion than Rabex5 alone (Delprato and Lambright, 2007; Lippé et al., 2001). These data led to the formation of the current model that Rab5-GTP binds Rbpt5 on endosomes and thus co-recruits its associated GEF Rabex5 resulting in further Rab5 activation. In this manner, high Rab5 activity is maintained by a positive-feedback loop. Free Rabex5 has also been shown to bind to endosomes directly through an early-endosome-

Biozentrum, University of Basel, Klingelbergstrasse 70, Basel CH-4056, Switzerland.

*Author for correspondence (martin.spiess@unibas.ch)

Received 20 May 2015; Accepted 22 September 2015

Journal of Cell Science (2015) 128, 4126-4137 doi:10.1242/jcs.174664

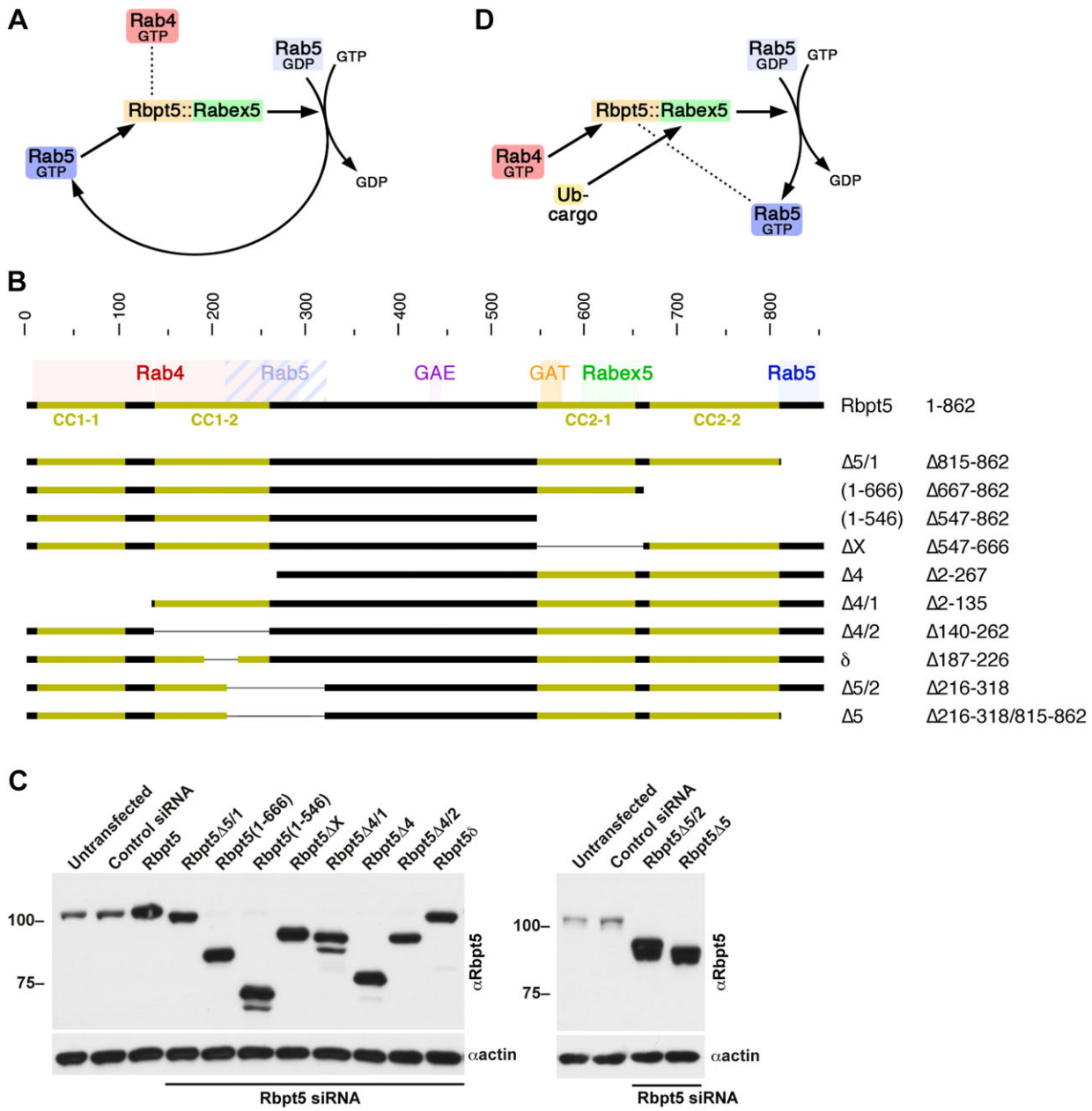

Fig. 1. Domain organization of wild-type Rbpt5 and deletion mutants. (A) Feedback model of Rbpt5 function. Rab5 recruits Rbpt5 with associated Rabex5, which activates more Rab5-GTP. Rbpt5 interacts with Rab4-GTP (dotted line). (B) Schematic representation of the sequence of Rbpt5. Coiled coil segments are shown in yellow. Colored backgrounds highlight the segments reported to interact with Rab4, Rab5, Rabex5, and the GAE and GAT domains of GGAs. Below, deletion mutants, their names and the deleted residues are listed. (C) Expression of wild-type and mutant Rbpt5 in transfected HeLa cells was assessed by immunoblot analysis. To distinguish between endogenous and exogenous protein, expression of endogenous Rbpt5 was silenced by siRNA before transfection. As a loading control, samples were blotted in parallel for actin. The position of molecular mass markers is indicated on the left (in kDa). (D) New model of Rbpt5 action. Rab4 and ubiquitylated cargo recruit Rbpt5–Rabex5 through binding sites in the respective subunits. Rabex activates Rab5, which binds to sites in Rbpt5 (dotted line).

targeting sequence (Zhu et al., 2007) or a ubiquitin-binding domain (Mattera and Bonifacino, 2008), independently of its GEF activity and of Rab5. This has been proposed as a mechanism to initiate the Rab5 activation loop (Zhu et al., 2007, 2010). The feedback loop is finally broken in the process of maturation from Rab5- to Rab7-dominated endosomes (Huotari and Helenius, 2011; Poteryaev et al., 2010; Rink et al., 2005). This Rab conversion involves a complex of SAND-1 (also known as Mon1A) and Ccz1 that is recruited by Rab5 and PI3P, and itself recruits Rab7 and somehow displaces Rabex5 from the membrane.

Rbpt5 also binds Rab4-GTP in the N-terminal third of the protein (Fig. 1B, top). Different studies have identified an interacting segment within residues 5–135 with coiled-coil domain CC1-1 (Vitale et al., 1998) or 140–294 with CC1-2 (Deneka et al., 2003; Korobko et al., 2005). The contribution of a Rab4-binding domain in Rbpt5 appeared to be reflected in an observed increase of Rab4/Rab5 double-positive endosomes, supporting the notion of Rbpt5 coordinating or coupling these two Rabs and their effector networks (De Renzis et al., 2002). Further binding sites have been identified in Rbpt5 for the γ-adaptin ear (GAE) domain of AP-1 clathrin

Journal of Cell Science (2015) 128, 4126-4137 doi:10.1242/jcs.174664

adaptors and GGAs (Golgi-localizing, γ-adaptin ear homology domain, ARF-binding proteins), and for the GGA-GAT domain (Deneka et al., 2003; Mattera et al., 2003; Zhu et al., 2004a).

In the present study, we analyzed the function of Rbpt5 in more detail by deletion of individual interaction domains as outlined in Fig. 1B and expression of the mutant proteins in HeLa cells. Some of our results clearly contradict the widely accepted feedback model in which Rab5 controls its own activity through Rbpt5–Rabex5. They rather indicate that Rbpt5 is recruited to early endosomes by Rab4 and by Rabex5 interacting with ubiquitylated cargo to activate Rab5 in a feed-forward manner. Overexpression of Rbpt5 appears to promote the formation of large endosomes with early and late endosomal characteristics, but is normally kept in check by Rab5-GTP.

RESULTS

Rbpt5 recruitment to endosomes does not require Rab5

Endogenous levels of Rbpt5 in HeLa cells were not detected by immunofluorescence microscopy with available antibodies (as in previous studies). However, transfected Rbpt5 was observed in the cytosol and on membrane structures containing internalized fluorescent Tf as a marker for early endosomes (Fig. 2A). Upon brief digitonin permeabilization of the plasma membrane before fixation, the cytosolic pool was lost and only endosome-bound Rbpt5 was retained (Fig. S1A). In the Rbpt5-expressing cells, the morphology of Tf-positive endosomes was unchanged as shown by quantification visualized by a box plot (Fig. 2F). Endosome sizes covered a wide size range, with most within 7–20 nm^2. Only when expression was further enhanced with butyrate, was significant enlargement observed, with most endosomes then being in the range of 14–75 nm^2 and a up to a maximum of ∼15 μm^2 (Fig. 2B,F). This treatment thus reproduced the effect observed in previous studies with strong overexpression using butyrate (Deneka et al., 2003) or using a vaccinia T7 RNA polymerase expression system (Stenmark et al., 1995).

Silencing of endogenous Rbpt5 expression by transfection of specific small interfering RNAs (siRNAs) did not noticeably affect Tf uptake, the morphology and distribution of Tf-positive endosomes, or the rate of Tf recycling as measured by automated quantitative fluorescence microscopy (Fig. S2). Similarly, overexpression of wild-type Rbpt5 only slightly reduced Tf recycling (consistent with Deneka et al., 2003).

For coexpression and colocalization analysis of two or more proteins, we used MultiLabel, a modular plasmid-based eukaryotic expression system (Kriz et al., 2010) that allows similar expression levels from identical promoters at a constant ratio in all transfected cells. Expression of Rabex5 (or mCherry-tagged Rabex5) alone (Fig. S1B) and – to an even higher extent – together with Rbpt5 induced the formation of large endosomes of up to ∼50 μm^2 (Fig. 2C,F), in agreement with previous reports. Coexpressed Rbpt5 and RFP-tagged Rab5 (isoform Rab5a) mostly colocalized on endosomes (Fig. 2D), as did Rbpt5 and citrine-tagged Rab4 (isoform Rab4a; Fig. 2E). Rab4 expression, both with and without Rbpt5, produced a subpopulation of enlarged endosomes of up to 14 μm^2 (Fig. 2E,F; Fig. S1D). In addition, Rab4 overexpression appeared to reduce the cytosolic pool of Rbpt5, suggesting that it might enhance membrane recruitment of Rbpt5 through the Rab4-binding domain(s).

To characterize the contributions of the Rbpt5 interactions with Rab4, Rab5 and Rabex5 to membrane recruitment of Rbpt5 and endosome size, we performed a deletion analysis testing the Rbpt5 mutants schematically illustrated in Fig. 1B. In Rbpt5Δ5/1, deletion of the C-terminal residues 815–862, which contain the best characterized Rab5-binding domain, did not affect the ability of the protein to dimerize, as shown by chemical crosslinking in intact cells and immunoblot analysis, in comparison to wild-type Rbpt5 (Fig. 3A). The expression levels of Rbpt5Δ5/1 (and of the other deletion mutants tested) were similar to those of transfected wild-type Rbpt5 (Fig. 1C). Unexpectedly, expressed Rbpt5Δ5/1 was still

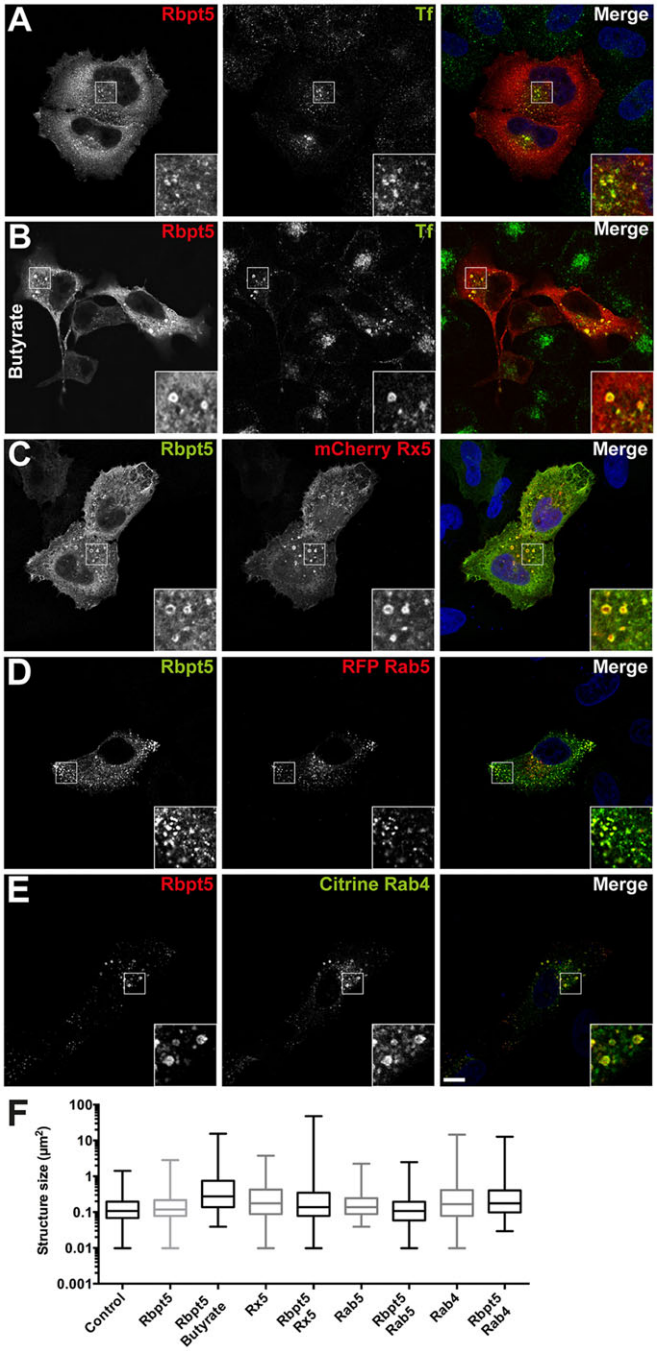

Fig. 2. Rbpt5 colocalizes with Tf-positive endosomes in transfected HeLa cells. (A,B) Rbpt5-transfected HeLa cells were not treated (A) or treated with butyrate to stimulate further overexpression of Rbpt5 (B). Fluorescent Tf was internalized for 1 h and the cells were fixed and stained for Rbpt5. (C–E) Rbpt5 was coexpressed with mCherry–Rabex5, RFP–Rab5 or Citrine–Rab4. Nuclei were stained with DAPI (blue). Scale bar: 10 μm. (F) Quantification of the size distribution of Tf- or Rbpt5-positive endosomes. Box plots show the median and the center 50% of values (interquartile range) in the box, with the whiskers representing the range.

Journal of Cell Science (2015) 128, 4126-4137 doi:10.1242/jcs.174664

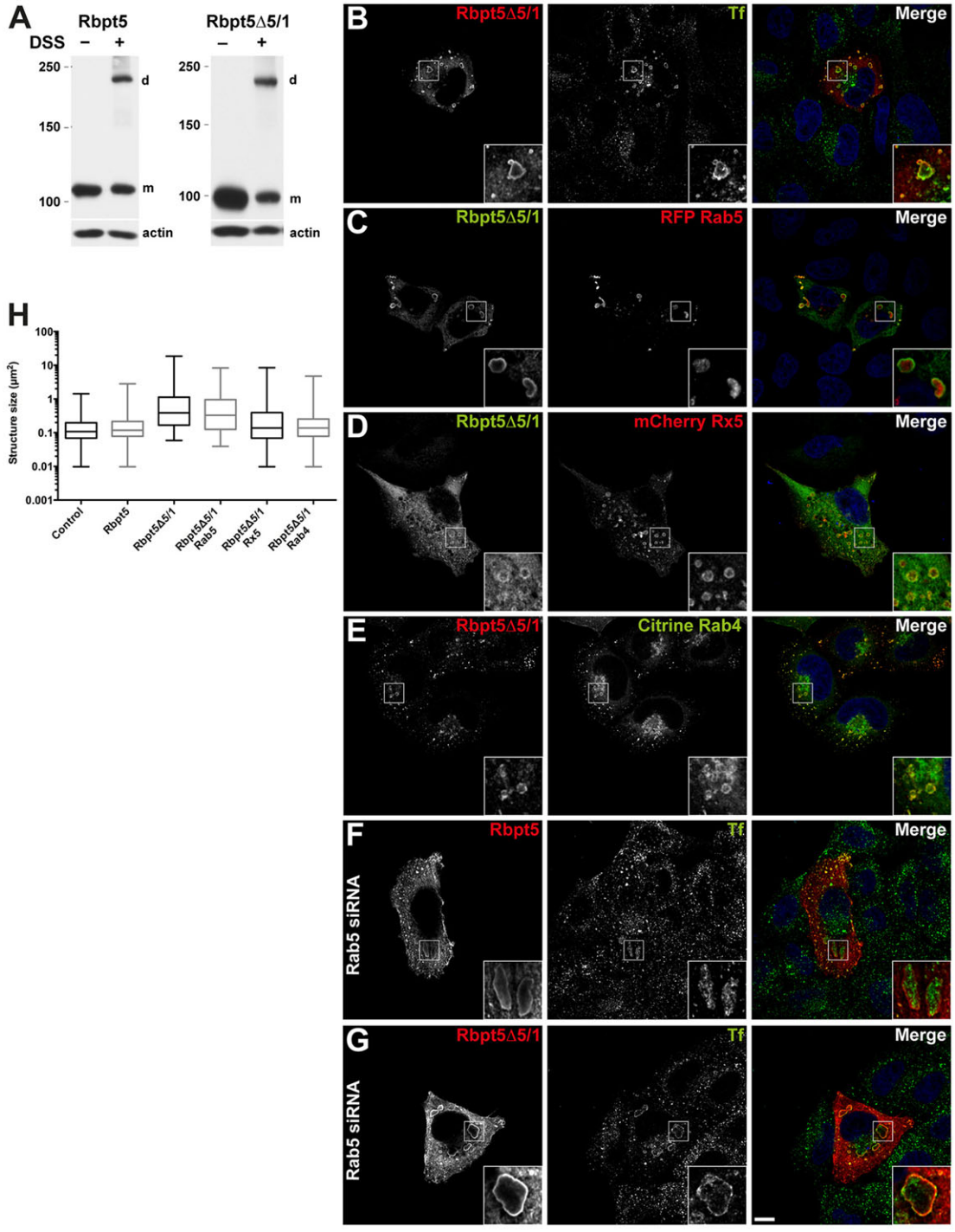

Fig. 3. Rbpt5Δ5/1 is still recruited to endosomes and induces their enlargement. (A) Cells expressing wild-type Rbpt5 or Rbpt5Δ5/1 were incubated with or without DSS, lyzed and analyzed by SDS gel electrophoresis and immunoblotting to evaluate crosslinking from monomers (m) to dimers (d). As a loading control, samples were blotted in parallel for actin. The position of molecular mass markers is indicated on the left (in kDa). (B) HeLa cells expressing Rbpt5Δ5/1 were loaded for 1 h with Tf before immunostaining. (C–E) Rbpt5Δ5/1 colocalized with RFP–Rab5, mCherry–Rabex5 (Rx5) and Citrine–Rab4, respectively. (F,G) Wild-type Rbpt5Δ5 or Rbpt5Δ5/1, respectively, colocalized with internalized fluorescent Tf in cells in which Rab5 expression was silenced by siRNA transfection. Knockdown efficiency is shown in Fig. S2. Nuclei were stained with DAPI (blue). Scale bar: 10 µm. (H) Quantification of the size distribution of endosomes. Box plots show the median and the center 50% of values (interquartile range) in the box, with the whiskers representing the range. Control and wild-type Rbpt5 are the same as in Fig. 2F for comparison.

recruited to Tf-containing endosomes (Fig. 3B), many of which in addition were enlarged in comparison to untransfected cells or cells expressing wild-type Rbpt5, some of them dramatically with sizes of up to ~20 µm^2 (Fig. 3H). A majority of cells that strongly expressed Rbpt5Δ5/1 produced giant structures of the dimensions >3 µm (67±3%, as opposed to 6±2% of cells strongly expressing wild-type Rbpt5; mean±s.d., n=3 independent experiments). This suggests that binding to Rab5 through the C-terminal domain is not necessary for membrane recruitment of Rbpt5 and might prevent Rbpt5-induced endosome enlargement.

Journal of Cell Science (2015) 128, 4126-4137 doi:10.1242/jcs.174664

Interestingly, cells producing giant Rbpt5Δ5/1-positive structures typically (i.e. in ∼75% of the cases) displayed perinuclear Tf-containing endosomes (most likely recycling endosomes) that were devoid of Rbpt5Δ5/1 (Fig. 3B). The mechanism causing this phenomenon is unclear. The giant Rbpt5Δ5/1-positive endosomes were still positive for Rab5, as was shown by coexpression with Rab5 (Fig. 3C). Surprisingly, however, Rab5 and Tf were frequently found inside these Rbpt5Δ5/1-positive membranes (Fig. 3B,C). In contrast, coexpressed Rabex5 and Rab4 decorated the Rbpt5Δ5/1 endosomes on the periphery and decreased endosome size to about the levels observed in cells expressing Rabex5 or Rab4 alone or in combination with wild-type Rbpt5 (Fig. 3D,E,H). Rab4 expression also appeared to reduce the cytosolic pool of Rbpt5Δ5/1, again suggesting improved recruitment to endosomes by increased Rab4 levels (Fig. 3E).

To directly assess the role of Rab5 in membrane recruitment of Rbpt5, Rab5a expression was knocked down by siRNA-mediated silencing. Endosome recruitment of both wild-type Rbpt5 and Rbpt5Δ5/1 remained unaffected, but induced dramatic endosome enlargement (Fig. 3F,G). These results argue against a role for Rab5 in recruiting Rbpt5 to endosomes as proposed by the feedback model. They also indicate that the formation of giant endosome structures by Rbpt5Δ5/1 is not dependent on Rab5-mediated endosome fusion. Again, in ∼45% of these cells, perinuclear Tf-positive, but Rbpt5-negative, endosomes were observed.

Rabex5 and its ubiquitin-binding domains are necessary for Rbpt5 recruitment

Further C-terminal truncation to also remove the coiled-coil region CC2-2 in Rbpt5(1–666) produced giant endosomes just as Rbpt5Δ5/1 (Fig. S3A). When in addition CC2-1, including the Rabex5-binding domain, was also deleted, the resulting protein Rbpt5(1–546) remained completely cytosolic, as reported previously (Vitale et al., 1998), and had no effect on the size of Tf-positive endosomes (Fig. S3B). The same phenotype was obtained when only CC2-1, the binding site of Rabex-5, was deleted in Rbpt5ΔX (Fig. 4A,J), suggesting that there is a role for Rabex5 in Rbpt5 recruitment. As expected, Rabex5 was not co-immunoprecipitated with Rbpt5ΔX (Fig. 4G), but Rbpt5ΔX was still able to dimerize as shown by crosslinking (Fig. 4H). Rbpt5ΔX was also capable of binding to GST–Rab4 and GST–Rab5 specifically in their GTP-bound forms (Fig. 4I). These controls argue against a general structural defect in Rbpt5ΔX causing the observed lack of membrane recruitment. Indeed, siRNA-mediated silencing of Rabex5 expression also abolished endosome recruitment of wild-type Rbpt5 (Fig. 4B), indicating that Rabex5 binding is required for membrane association.

Coexpression of Rabex5 with Rbpt5ΔX did not rescue membrane binding, even though the concomitant enlargement of the endosomes reflects Rab5 activation (Fig. 4C). Interestingly, however, coexpression of Rab5 induced minimal membrane recruitment of Rbpt5ΔX (Fig. 4D), whereas Rab4 coexpression fully restored membrane binding (Fig. 4E).

Rabex5 has been shown to bind to endosomes through an N-terminal ubiquitin-binding domain (Mattera and Bonifacino, 2008). Rabex5ΔUb, in which the N-terminal 75 residues, including both the ubiquitin-binding zinc finger and the 'motif interacting with ubiquitin' (MIU) domain were deleted and replaced by a HA tag, remained cytosolic when expressed in HeLa cells (Fig. S4; in agreement with Mattera and Bonifacino, 2008). When coexpressed with wild-type Rbpt5, it also prevented Rbpt5 from localizing to endosomes (Fig. 4F). This indicates that Rabex5 connects Rbpt5 to ubiquitylated cargo in early endosomes.

Rab4 is required for Rbpt5 recruitment through two distinct N-terminal domains

To analyze the involvement of Rab4 in recruiting Rbpt5 we used construct Rbpt5Δ4, where the N-terminal 285 residues, including all published Rab4-binding sequences, are deleted. To assess its folding state, we tested for co-immunoprecipitation of Rbpt5 with Rabex5, the binding of which is crucially dependent on coiled-coil formation in segment CC2-1. As shown by the immunoblot analysis in Fig. 5A, Rabex5 was co-immunoprecipitated with Rbpt5Δ4 and vice versa as efficiently as the wild-type protein, demonstrating efficient complex formation. However, Rbpt5Δ4 was not recruited to endosomes at all and remained cytosolic (Fig. 5B). Upon digitonin permeabilization, no signal was retained on cellular membranes (Fig. 5C). Coexpression of Rab4 could not rescue membrane recruitment of Rbpt5Δ4 (Fig. 5D), but overexpression of Rabex5 (Fig. 5E) or even Rab5 could (Fig. 5F).

To more directly assess the role of Rab4, we analyzed the effect of silencing Rab4 on the membrane recruitment of wild-type Rbpt5. Rab4 knockdown completely prevented membrane binding of full-length Rbpt5 (Fig. 5G). These findings indicate that endosome recruitment of Rbpt5 is primarily mediated by Rabex5 and Rab4-GTP.

Although previous studies agree that the N-terminal third of Rbpt5 binds to Rab4 as detected by yeast two-hybrid analysis (Korobko et al., 2005; Vitale et al., 1998) or GST–Rab4 pulldown experiments (Deneka et al., 2003), they differ on the location of the interacting sequence(s) within this segment, suggesting that these are either residues 5–135, including the coiled-coil domain CC1-1 (Vitale et al., 1998), or residues 140–295, including CC1-2 (Deneka et al., 2003; Korobko et al., 2005). Accordingly, we analyzed the deletion constructs Rbpt5Δ4/1 lacking residues 2–135 and Rbpt5Δ4/2 lacking residues 140–262 (illustrated in Fig. 1A) and found both to be efficiently recruited to Tf-containing endosomes (Fig. 6A,B), suggesting that both segments are able to bind Rab4 independently.

To test this directly, we performed pulldown experiments using an immobilized GST–Rab4 fusion protein. Expressed wild-type Rbpt5, but not Rbpt5Δ4, specifically interacted with GST–Rab4 bound to the GTP analog GMP-PNP and not to the GDP-bound form (Fig. 6H, top), confirming the presence of Rab4-binding site(s) in the N-terminal third of the protein. Rbpt5Δ4/1 also bound very efficiently, indicating a strong binding site in CC1-2. Surprisingly, Rbpt5Δ4/2 did not sufficiently bind GST–Rab4 to produce a signal. The recruitment phenotype of Rbpt5Δ4/2 together with the lack of recruitment upon Rab4 silencing and the positive yeast two-hybrid signal for CC1-1 (Vitale et al., 1998) suggest either a second Rab4 interaction sequence of low affinity (at least under *in vitro* conditions) or interaction with another component that itself depends on Rab4 for endosome localization or activity. All these mutants still bound to GST–Rab5 (Fig. 6H, bottom).

Deletion of either Rab5-binding domain induces giant membrane structures positive for early and late markers

The two deletions Rbpt5Δ4/1 and Rbpt5Δ4/2 differed in that only the latter caused the formation of giant endosomes (Fig. 6G), frequently containing Tf in their lumen rather than on the periphery, reminiscent of the phenotype of Rbpt5Δ5/1 (Fig. 3A). The deletion in Rbpt5Δ4/2 indeed overlaps with a second reported Rab5-interacting segment (residues 216–318; Korobko et al., 2006) that might be inactivated by the deletion in Rbpt5Δ4/2. Expression of Rbpt5δ, a natural splice variant lacking residues 187–226, which hardly cut into the Rab5-interacting segment, did not cause

Journal of Cell Science (2015) 128, 4126-4137 doi:10.1242/jcs.174664

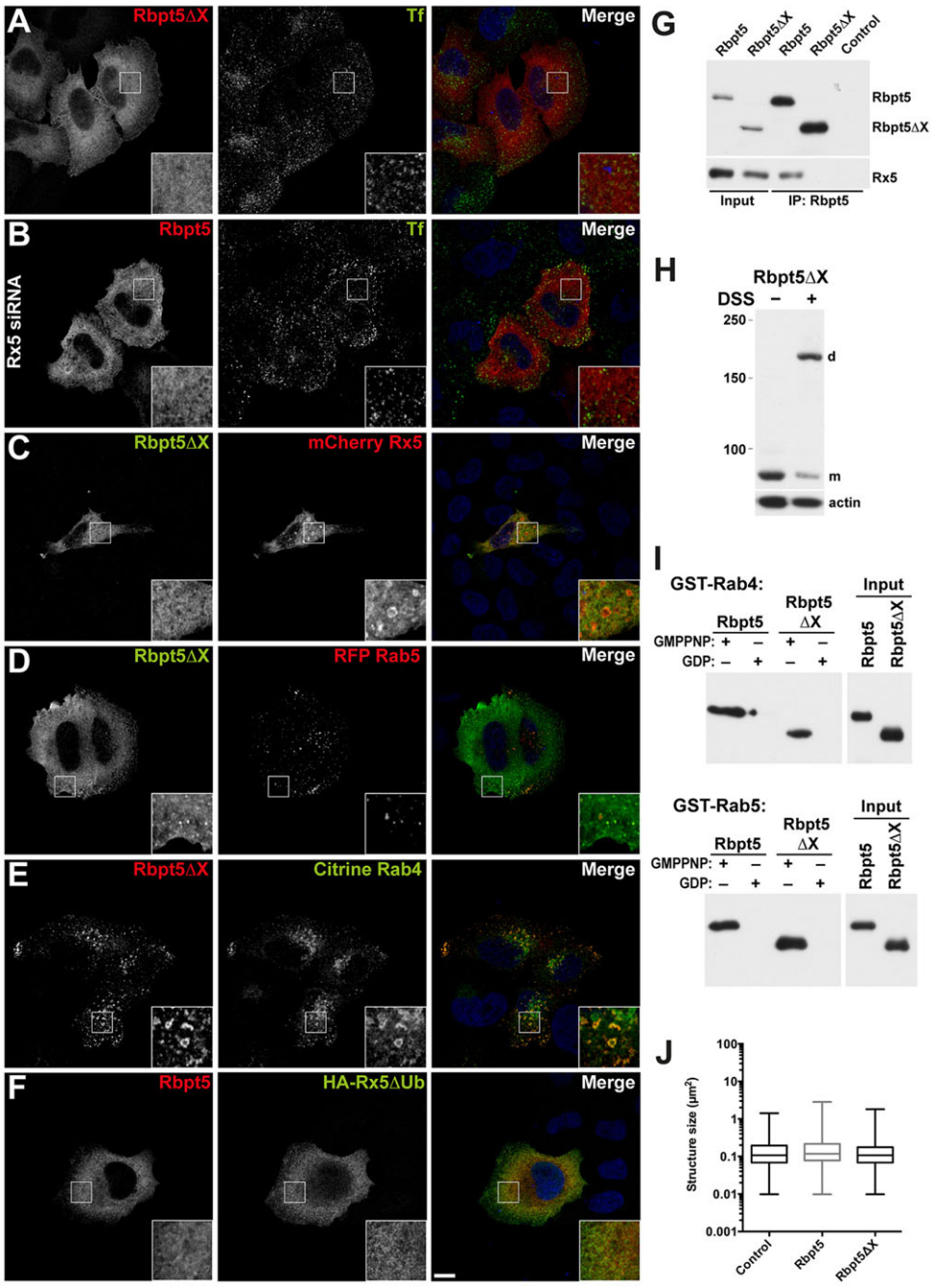

Fig. 4. Rabex5 is required for Rbpt5 recruitment to endosomes.
(A) Immunofluorescence staining of Rbpt5ΔX in cells loaded with fluorescent Tf. (B) Wild-type Rbpt5 was immunostained in Tf-loaded cells in which Rabex5 expression was silenced by siRNA transfection. Knockdown efficiency is shown in Fig. S2. (C–E) Rbpt5ΔX colocalized with mCherry–Rabex5 (Rx5), RFP–Rab5 or Citrine–Rab4, respectively. (F) Wild-type Rbpt5 was expressed with the HA-tagged Rabex5 mutant lacking the N-terminal ubiquitin-binding domains (HA–RxΔUb). Nuclei were stained with DAPI (blue). Scale bar: 10 µm. (G) Lysates of cells expressing wild-type Rbpt5 or Rbpt5ΔX or untransfected cells (control) were immunoprecipitated (IP) with anti-Rbpt5 antibodies before blotting for Rbpt5 and Rabex5 to assess the efficiency of Rabex5 binding. 6% of input material was loaded as controls. (H) Cells expressing Rbpt5ΔX were incubated with or without DSS, lyzed and analyzed by SDS gel electrophoresis and immunoblotting to evaluate crosslinking from monomers (m) to dimers (d), as in Fig. 3A. (I) Bacterially expressed GST–Rab4 and GST–Rab5 were purified on glutathione–Sepharose, loaded with GMP-PNP or GDP, and incubated with cytosol of HeLa cells expressing wild-type Rbpt5 or Rbpt5ΔX. Beads were washed, and bound protein was eluted and visualized by immunoblot analysis. 10% input cytosols were analyzed in parallel as loading controls. (J) Quantification of the size distribution of endosomes upon expression of Rbpt5ΔX. Box plots show the median and the center 50% of values (interquartile range) in the box, with the whiskers representing the range. Control and wild-type Rbpt5 are the same as in Fig. 2F for comparison.

endosome enlargement (Fig. 6C,G). Deletion of the Rab5-interacting segment 216–318 in Rbpt5Δ5/2 also produced giant unshapely endosomes (in 71±1% of overexpressing cells; mean± s.d., n=3 independent experiments) containing Tf and coexpressed Rab5 in internal structures (Fig. 6D,E), whereas coexpressed Rab4 reduced the endosomes to round structures of intermediate size decorated with Rbpt5Δ5/2 and Rab4 on the periphery (Fig. 6F).

Pulldown experiments with GST–Rab5 confirmed that Rbpt5 constructs containing either one of the two Rab5 interaction segments (Rbpt5Δ5/1 and Rbpt5Δ5/2) bound Rab5-GMP-PNP (Fig. 7A, top). Deletion of both sites in Rbpt5Δ5 (Fig. 1), however, entirely abolished binding to Rab5. The Rab4-binding site in CC1-2 adjacent to the N-terminal Rab5 interaction motif was still intact, given that all three Δ5 mutants could be pulled down with GST–Rab4 (Fig. 7A, bottom).

The C-terminal Rab5-binding site was clearly the more potent one of the two *in vitro*. *In vivo*, however, deletion of either site alone produced the same phenotype. In addition to the early endosomal markers Tf and Rab5, the Rbpt5Δ5/1- and Rbpt5Δ5/2-positive giant endosomes were also stained for markers typical of late endosomes, such as CHMP2B (also known as VPS2B), a component of the ESCRTIII complex involved in formation of intraluminal vesicles, GFP–Rab7 (surprisingly inside the structures) and Lamp1 (Fig. 7B–D). To test for an endocytosed cargo delivered to late endosomes on the way to lysosomes, fluorescent EGF was internalized for 30 min. Given that uptake in HeLa cells was minimal, the experiment was performed in A431 cells expressing more EGF receptors. In A431 cells, the phenomena produced by the Rbpt5 mutants shown above in HeLa cells were reproduced (Fig. S4). Internalized EGF was also detected inside the giant

Journal of Cell Science (2015) 128, 4126-4137 doi:10.1242/jcs.174664

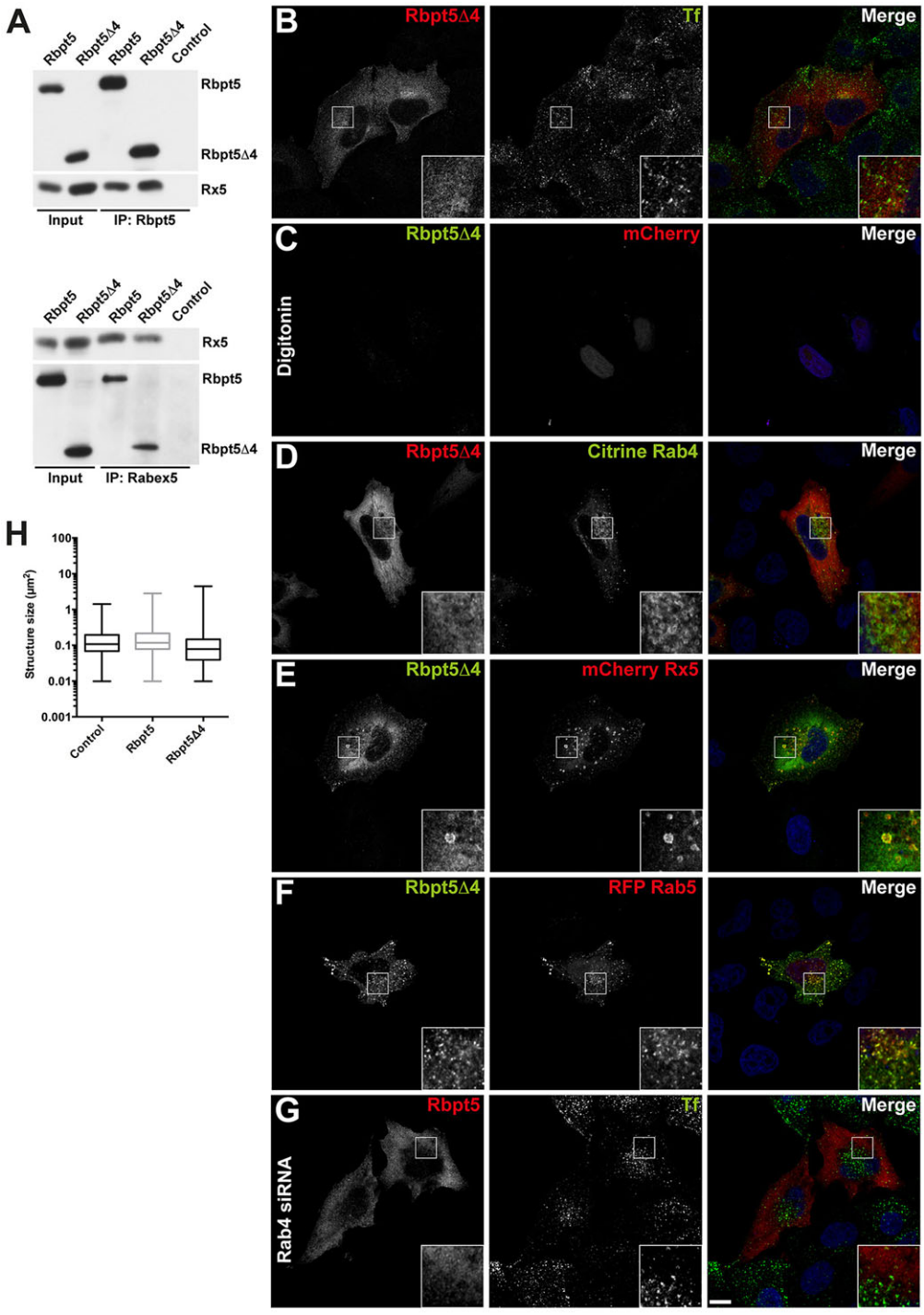

Fig. 5. Rab4 is required for Rbpt5 recruitment to endosomes.
(A) Lysates of cells expressing wild-type Rbpt5 or Rbpt5Δ4 or untransfected cells (Control) were immunoprecipitated with anti-Rbpt5 antibodies (top) or with anti-Rabex5 antibodies (bottom) before blotting for Rbpt5 and Rabex5 to assess the efficiency of Rabex5 binding and thus dimerization. 6% of input material was loaded as controls.
(B) Immunofluorescence staining of Rbpt5Δ4 in cells loaded with fluorescent Tf. (C) Expressed Rbpt5Δ4 is completely released upon digitonin permeabilization before fixation. mCherry, which is retained in the nuclei, was coexpressed with Rbpt5Δ4 to identify transfected cells.
(D–F) Rbpt5Δ4 was coexpressed with Citrine–Rab4, mCherry–Rabex5 or RFP–Rab5, respectively. Rabex5 and Rab5 overexpression partially rescued Rbpt5Δ4 membrane recruitment.
(G) Endosome recruitment of wild-type Rbpt5 was abolished when Rab4 expression was silenced by siRNA. Nuclei were stained with DAPI (blue). Scale bar: 10 μm. (H) Quantification of the size distribution of endosomes upon expression of Rbpt5Δ4. Box plots show the median and the center 50% of values (interquartile range) in the box, with the whiskers representing the range. Control and wild-type Rbpt5 are the same as in Fig. 2F for comparison.

endosomes (Fig. 7E). Tf was observed in small and large endosomes after 1 h of endocytosis (Fig. 7F). After a further 20-min chase, Tf had recycled out of peripheral small endosomes, but was still trapped within the giant Rbpt5Δ5/2-induced endosomes (Fig. 7G).

Interestingly, the double deletion Rbpt5Δ5 also bound to membranes and produced giant structures (in 65±3% of overexpressing cells; mean±s.d., n=3 independent experiments) that were positive for the late endosomal markers CHMP2B and Rab7, but not for the early markers Tf and Rab5 (Fig. 8). This indicates that the phenotype of the double deletion Rbpt5Δ5 that lacks any interaction with Rab5, differs from those of the single mutants Rbpt5Δ5/1 and Rbpt5Δ5/2. All deletion constructs affecting Rab5 binding shared the phenomenon of containing perinuclear Tf-positive endosomes, negative for the respective Rbpt5 mutants in ∼75% of the cells (also visible in Figs 3B, 6D, 8A; Fig. S4D,F). This phenotype is also reflected in the extent of colocalization of Rbpt5 and Tf with Pearson's coefficients of 0.65±0.03 for wild-type Rbpt5 and 0.39±0.12 for Rbpt5Δ5/2 (mean±s.d., n=6), for example.

DISCUSSION

Our experiments reproduce previously published data, but – extended by a detailed deletion analysis and with additional information on Rbpt5 interactors that has been accumulated in recent years – they do

Journal of Cell Science (2015) 128, 4126-4137 doi:10.1242/jcs.174664

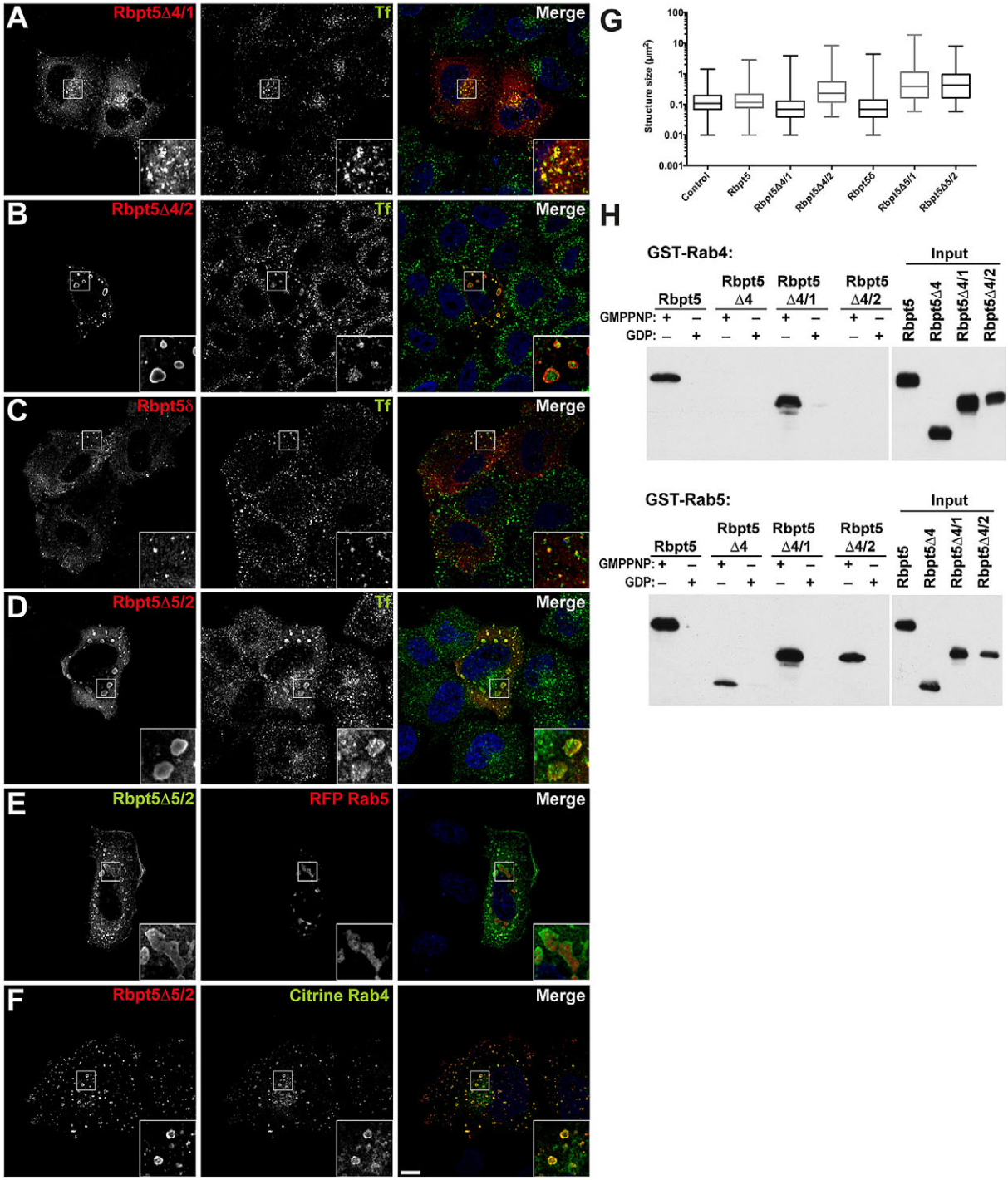

Fig. 6. Rbpt5 contains N-terminal binding sites for Rab4 and Rab5. (A–D) Deletion mutants Rbpt5Δ4/1, Rbpt5Δ4/2, Rbpt5δ and Rbpt5Δ5/2 were expressed and co-stained with internalized fluorescent Tf. (E,F) Rbpt5Δ5/2 was coexpressed with RFP–Rab5 and Citrine–Rab4. Nuclei were stained with DAPI (blue). Scale bar: 10 μm. (G) Box plots show the median and the center 50% of values (interquartile range) in the box, with the whiskers representing the range. Quantification of the size distribution of endosomes. Control and wild-type Rbpt5 are the same as in Fig. 2F for comparison. (H) Bacterially expressed GST–Rab4 and GST–Rab5 were purified on glutathione–Sepharose, loaded with GMP-PNP or GDP, and incubated with cytosol of HeLa cells expressing wild-type or the indicated Rbpt5 mutants. Beads were washed, and bound protein were eluted and visualized by immunoblot analysis. 10% input cytosols were analyzed in parallel as loading controls.

not support the positive-feedback model for Rbpt5 function. Rather than Rab5-GTP recruiting Rbpt5–Rabex5 to promote further Rab5 activation, our results show that endosome recruitment of Rbpt5 is mediated by Rab4 and Rabex5 (Fig. 1D). Binding to Rab4 or a Rab4-dependent factor by at least one of two independent binding sites, in CC1-1 and CC1-2, respectively, and binding to Rabex5 through CC2-1 are necessary for membrane association. Rbpt5 thus rather fits into the activation coupling mode of action in which Rab4 promotes activation of Rab5 on early endosomes. This could explain the earlier observation that Rbpt5 overexpression caused an apparent increase in

Journal of Cell Science (2015) 128, 4126-4137 doi:10.1242/jcs.174664

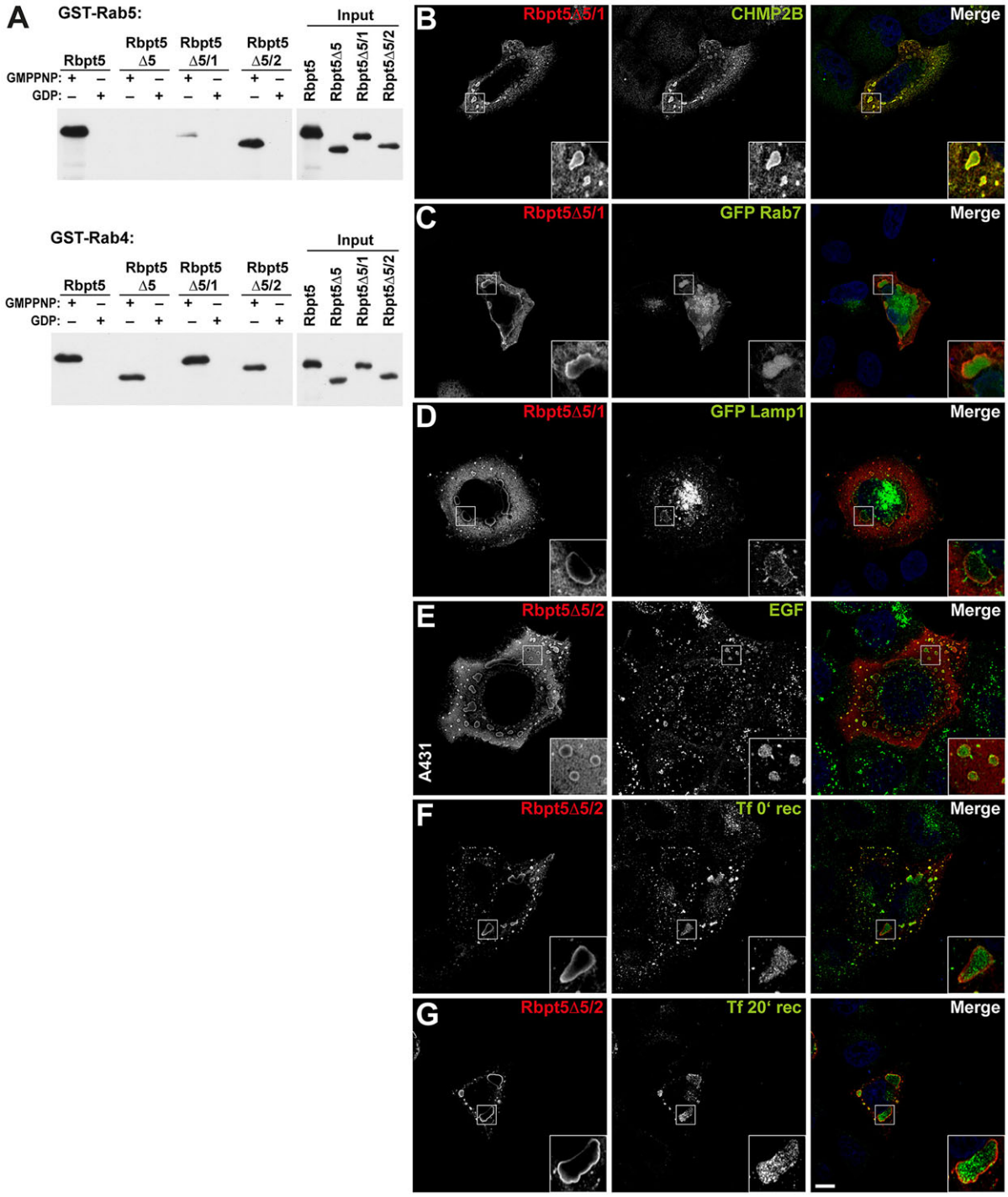

Fig. 7. Enlarged endosomes induced by Rbpt5Δ5/1 or Rbpt5Δ5/2 contain late endosomal markers. (A) Binding of wild-type or the indicated Rbpt5 mutants to GMP-PNP- or GDP-loaded GST–Rab4 and GST–Rab5 was analyzed as in Fig. 6H. (B–D) Rbpt5Δ5/1 expressed in HeLa cells was co-stained with the endogenous ESCRT component CHMP2B, with co-transfected GFP–Rab7 or GFP–Lamp1, respectively. (E) A431 cells expressing Rbpt5Δ5/2 were incubated with fluorescent EGF for 30 min before fixation and analysis. (F,G) HeLa cells expressing Rbpt5Δ5/2 were loaded with fluorescent Tf for 1 h at 37°C and acid-stripped to retain only internalized Tf (0′ rec; F). Cells were then incubated at 37°C for another 20 min and surface-stripped again to assess Tf recycling (20′ rec; G). Nuclei were stained with DAPI (blue). Scale bar: 10 µm.

Rab4/Rab5 double-positive endosomes (De Renzis et al., 2002). Rab4-mediated activation of Rab5 and thus of endosome fusion is a likely cause of the observed mild increase in the size of Tf-positive endosomes upon overexpression of Rab4.

Overexpression of Rab4 or Rabex5 could rescue recruitment of Rbpt5 mutants lacking binding sites for Rabex5 or Rab4, respectively. Rab5 overexpression could also, but only partially, rescue membrane binding of Rbpt5ΔX and Rbpt5Δ4, highlighting the fact that Rbpt5, Rabex5, Rab4-GTP and Rab5-GTP participate in a complex network of interactors stabilizing each other.

Rabex5 contains an ubiquitin-interaction motif and has been shown to be recruited to ubiquitylated endosomal cargo (Mattera

Journal of Cell Science (2015) 128, 4126-4137 doi:10.1242/jcs.174664

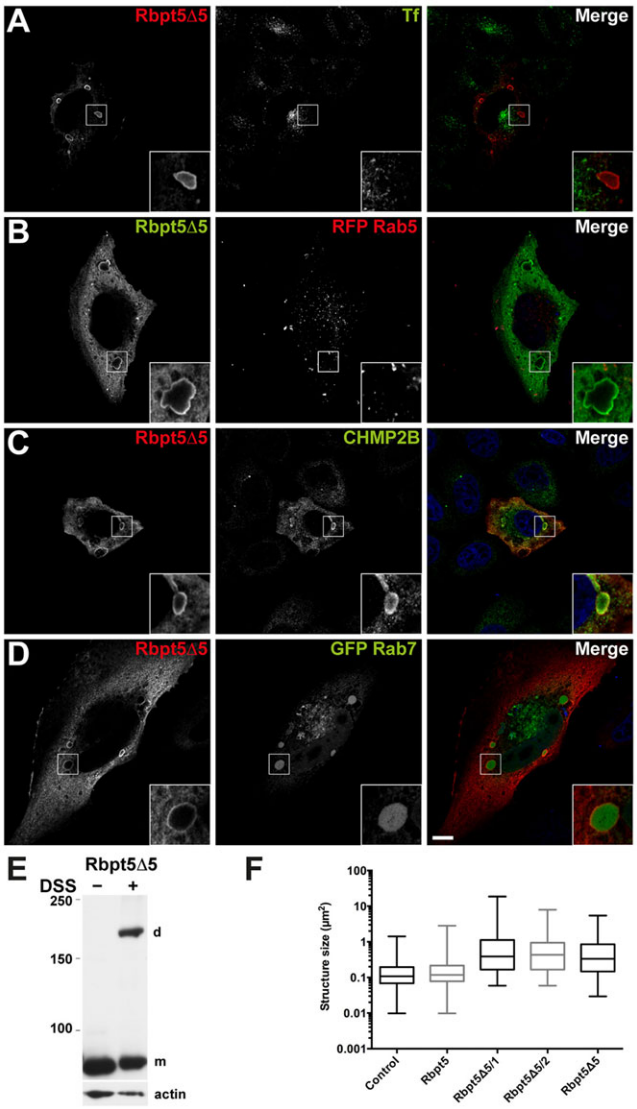

Fig. 8. Deletion of both Rab5-binding domains in Rbpt5 induces giant endosomes with late endosomal properties. (A–D) Cells expressing Rbpt5Δ5 were co-stained with internalized fluorescent Tf, and for coexpressed RFP–Rab5, endogenous CHMP2B or GFP–Rab7, respectively. Nuclei were stained with DAPI (blue). Scale bar: 10 µm. (E) Cells expressing Rbpt5Δ5 were incubated with or without DSS, lyzed, and analyzed by SDS gel electrophoresis and immunoblotting to evaluate crosslinking from monomers (m) to dimers (d). Actin was blotted as a loading control. The position of molecular mass markers is indicated on the left (in kDa). (F) Quantification of the size distribution of endosomes. Box plots show the median and the center 50% of values (interquartile range) in the box, with the whiskers representing the range. Control and wild-type Rbpt5 are the same as in Fig. 2F for comparison.

and Bonifacino, 2008). The specificity of Rbpt5 targeting is thus to endosomes positive for Rab4-GTP and for ubiquitylated cargo. The GEF activity of bound Rabex5 also keeps these endosomes positive for Rab5-GTP. Endosomes or endosomal subcompartments containing ubiquitylated cargo are destined for maturation to late endosomes by forming intraluminal vesicles where the ubiquitylated cargo is sequestrated for subsequent degradation. The concomitant loss of surface-bound ubiquitin thus offers itself as a potential mechanism to release Rbpt5–Rabex5 from the surface of maturing endosomes resulting in the loss of Rab5 activation and early endosome identity. Another mechanism is the loss of Rab4-GTP from the membranes.

Endosome maturation appears to be dysregulated upon expression of Rbpt5 mutants lacking either one of the two Rab5 interaction segments. They caused the formation of dramatically enlarged structures containing markers of both early and late endosomes. This is reminiscent of the giant endosomes produced in cells overexpressing constitutively active Rab5 (Hirota et al., 2007; Wegener et al., 2010). Here, the formation of enlarged multivesicular early-late chimeras was explained by the persistence of active Rab5 on maturing endosomes that allows late endosomes to retain early endosomal features including the ability to fuse with early endosomes. However, the enlargement of endosomes induced by expression of Rbpt5 lacking Rab5-binding sequences is not due to Rab5-mediated membrane fusion. Giant endosomes were also produced by wild-type Rbpt5 when Rab5 expression was silenced. The phenotype therefore cannot be explained by inhibition of membrane fusion due to Rbpt5 binding to Rab5, but rather the opposite: Rbpt5 overexpression appears to promote the formation of large, frequently malformed, structures with early and late markers, unless it is restrained by Rab5 binding to both binding sites. In addition, some endosomal markers that normally remain peripheral were found inside the structures produced by the Rbpt5Δ5 mutants, but not in those produced by dominantly active Rab5. The mechanism for this phenomenon is unclear.

One might speculate that Rbpt5 at physiological concentrations contributes to maturation from early to late endosomes, possibly by interacting with yet unknown partners. Rab5-GTP, the levels of which are initially kept high by Rabex5, might inhibit the contribution of Rbpt5 until its levels drop, for example upon inactivation through increased GAP activity (Haas et al., 2005). Finally, Rbpt5–Rabex5 might be released from the progressing endosome either when the ubiquitylated cargo disappears from its surface upon deubiquitylation and internalization, or when Rab4-GTP levels go down.

Although we do not understand in detail how Rbpt5 mediates the observed changes in endosome morphology and composition when overexpressed in the absence of Rab5 or the Rab5-interaction domains, our results shed new light on the mechanism of Rbpt5 membrane recruitment by Rabex5 binding to ubiquitylated cargo and by Rab4-GTP in a feed-forward manner.

MATERIALS AND METHODS

Expression plasmids

The cDNAs encoding human Rbpt5 (from Marino Zerial, Max Planck Institute, Dresden, Germany), Rabex5 (amplified from a mouse brain cDNA library and fused to an HA epitope tag), human Rab4a (from Peter van der Sluijs, University of Utrecht, Germany), and human Rab5a (from Elizabeth Smythe, University of Sheffield, UK) were cloned into pcDNA3 (Invitrogen). Rbpt5 and Rx5 mutants were generated by PCR. All constructs were confirmed by sequencing.

For consistent coexpression of multiple proteins, we used the MultiLabel system described by Kriz et al. (2010). Wild-type and mutant Rbpt5 in pcDNA3 were amplified from the CMV promoter to the poly(A) sequence and cloned into pSI-DST2cx donor vector. Rab4, Rab5 and Rabex5 were ligated into the acceptor vectors pSI-AAL6 or pSI-AAR6 for N-terminal fusion of an mCitrine, mCherry or RFP tag, respectively. Acceptor plasmids (containing a pUC origin of replication) were propagated in UT580 cells, and donor plasmids (with an R6Kγ origin of replication) were propagated in Pir1 cells (Invitrogen). After Cre/LoxP recombination (New England BioLabs), the plasmids were transformed into UT580 cells by electroporation and plated on LB agar plates containing 50 µg/µl carbenicillin and 50 µg/µl spectinomycin.

Cell culture and transfection

HeLa α and A431 cells were grown in Dulbecco's modified Eagle's medium (DMEM) supplemented with 10% fetal calf serum (FCS), 100 units/ml

Journal of Cell Science (2015) 128, 4126-4137 doi:10.1242/jcs.174664

penicillin, 100 units/ml streptomycin and 2 mM L-glutamine at 37°C in 7.5% and 5% CO_2, respectively. Cells were transiently transfected using Fugene HD (Promega).

For RNA interference experiments, cells were reverse-transfected with 20 nM ON-TARGETplus human Rbpt5 siRNA (3′UTR), ON-TARGETplus SMARTpool human Rabex5, ON-TARGETplus SMARTpool human Rab4a, ON-TARGETplus SMARTpool human Rab5a or ON-TARGETplus non-targeting control pool siRNA (Dharmacon Thermo Scientific) using Lipofectamine RNAiMAX (Invitrogen). Cells were used after 3 days. For some experiments, the cells were transfected with expression plasmids using Fugene HD (Promega) after 1 day and cultured for another 2 days. Protein silencing was tested by immunoblot analysis. Butyrate-treated cells received 1 mM sodium butyrate 18 h before experiments to induce expression of cytomegalovirus (CMV)-driven constructs. GFP–Rab7a and GFP–Lamp1 were expressed using the BacMam baculovirus-based non replicative expression system (Invitrogen). Rbpt5-transfected cells were infected for GFP–Rab7a or GFP–Lamp1 expression 12 h before fixation.

Immunofluorescence

Transfected cells were grown on coverslips for 48 h. For transferrin staining, cells were allowed to internalize 20 µg/ml Alexa-Fluor-tagged transferrin (Invitrogen) in medium supplemented with 20 mM HEPES for 1 h at 37°C. Cells were fixed with 3% paraformaldehyde for 10 min at room temperature and quenched for 5 min with 50 mM NH_4Cl. In some experiments, the cells were pre-permeabilized with 40 µg/ml digitonin (Serva) in 110 mM potassium acetate, 20 mM HEPES and 2 mM $MgCl_2$ for 5 min at 4°C to release free cytosolic proteins.

Fixed cells were washed with PBS, permeabilized with 0.1% Triton X-100 for 10 min, blocked with 1% BSA in PBS for 15 min, incubated for 2 h with primary antibodies in PBS with BSA, washed and stained for 30 min with fluorescently tagged secondary antibodies in PBS with BSA. After a 5-min staining with DAPI and several washes with PBS, coverslips were mounted in Fluoromount-G (Southern Biotech). Staining patterns were analyzed using an upright Zeiss LSM700 confocal microscope. Images of single confocal planes are shown. All immunofluorescence experiments were repeated at least three times.

Endosome sizes were measured in four representative cells per condition containing between 900 and 1100 structures for normal-sized endosomes and 300–400 structures for Rbpt5 mutants causing giant endosomes. Endosome size was measured in the Rbpt5 channel and, for control cells, in the Tf channel. Images were analyzed with Bregman segmentation using the Mosaic plugin in Fiji as implemented by Aurélien Rizk (Rizk et al., 2014). Background was subtracted with a rolling ball radius of 10 pixels and cell masks were set to 0.075 to identify transfected cells. The resulting size values in pixel were translated into μm^2 and illustrated as box plots with Prism6. A box plot depicts 50% of the values in the middle box plus minimum and maximum values on both sides. The frequency of giant membrane structures with dimensions >3 µm was quantified by counting 50–100 overexpressing cells each in three experiments using a Zeiss Axioplan 2 epifluorescence microscope with a Leica DFC420C imaging system.

To quantify colocalization of wild-type Rbpt5 and Rbpt5Δ5/2 with Tf, images were acquired using an inverted Zeiss LSM700 confocal microscope (*z*-stack oversampling at 0.13-µm intervals and 0.04-µm pixel size, deconvoluted with Huygens software, and analyzed using the JACoP plugin in Fiji or ImageJ according to Bolte and Cordelières (2006) to determine the Pearson's coefficients.

Crosslinking and co-immunoprecipitation

To test dimer formation of wild-type or mutant Rbpt5, transfected cells were incubated with 0.1 mM disuccinimidyl suberate (DSS; ProteoChem) in PBS for 45 min at room temperature followed by quenching with 50 mM Tris-HCl pH 7.5 for 15 min. The cells were harvested in lysis buffer (0.5% Na-deoxycholate, 1% Triton X-100, 2 mM PMSF, protease inhibitor cocktail) for 1 h at 4°C and subjected to immunoblot analysis.

Alternatively, transfected cells expressing wild-type or mutant Rbpt5 and HA–Rabex5 were lysed 48 h post-transfection with lysis buffer at 4°C. Post-nuclear supernatants were incubated with anti-Rbpt5 or anti-HA overnight at 4°C, and antigen–antibody complexes were collected with protein-A–Sepharose for 2 h, washed four times with lysis buffer and PBS, and subjected to immunoblot analysis.

GST pulldown assay

Escherichia coli Rosetta cells were grown to express GST–Rab4 (isoform a) or GST–Rab5 (isoform a) in pGEX-4T-2 and the protein was purified with 4 ml glutathione–Sepharose-4B, according to manufacturer's instructions (GE Healthcare). Pulldown assays with GMP-PNP- or GDP-loaded GST–Rab4 or GST–Rab5 were performed as described previously (De Renzis et al., 2002). Cytosol was prepared from one 10-cm dish of transfected HeLa α cells after 48 h by scraping into 0.5 mM EDTA pH 8.0, pelleting and homogenization in 400 µl of 10 mM HEPES-NaOH pH 7.2 and 1 mM KCl with ten strokes of a motorized glass-Teflon homogenizer. The supernatant, after centrifugation at 150,000 ***g*** for 1 h at 4°C in a Beckman TLA-100 rotor, was used for GST pulldowns. Bound proteins were analyzed by SDS gel electrophoresis and immunoblotting.

Tf recycling and EGF uptake

Tf recycling was quantitatively assessed as described by Hirschmann et al. (2015). Briefly, transfected cells grown in flat clear-bottom black polystyrene TC-treated microplates (Corning Life Sciences) were starved for 2 h in uptake medium (medium supplemented with 20 mM HEPES pH 7.5), incubated for 1 h at 37°C with 50 µg/ml Alexa-Fluor-tagged transferrin in uptake medium, and washed three times with ice-cold PBS and twice with stripping buffer (150 mM NaCl, 50 mM Na-acetate, pH 3.5) to release surface transferrin. The cells were then quickly warmed to 37°C and internalized transferrin was chased for up to 20 min in uptake medium supplemented with 50 mM deferoxamine mesylate salt (Sigma). Cells were fixed with 3% paraformaldehyde in PBS, quenched with 50 mM NH_4Cl in PBS for 5 min, permeabilized with 0.1% Triton X-100 for 5 min, and stained with 1 unit/ml Alexa-Fluor-tagged phalloidin (Dyomics) and 10 µM bisbenzimide H33342 (Hoechst) for 30 min. Image acquisition was performed automatically with an ImageXpress Micro (Molecular Devices) and image analysis was performed with CellProfiler (Carpenter et al., 2006).

To observe endocytosed EGF, transfected A431 cells grown on coverslips were washed with pre-chilled, serum-free growth medium supplemented with 20 mM HEPES, pH 7.2. The coverslips were then incubated for 30 min at 4°C in serum-free growth medium containing 1% BSA, 20 mM HEPES, pH 7.2, and 2 µg/ml Alexa-Fluor-488–EGF (Invitrogen), washed three times in ice-cold PBS to remove excess ligand and transferred into pre-warmed growth medium. The cells were chased at 37°C with 5% CO_2 for 30 min and then fixed with 3% paraformaldehyde and processed for immunofluorescence.

Antibodies

Mouse anti-Rbpt5 (BD Transduction Laboratories) and rabbit anti-HA antibodies (1:1000; Abcam) were used for immunofluorescence and immunoblotting, rabbit anti-CHMP2B (1:200; Abcam) were used for immunofluorescence, mouse anti-Rabex5 antibodies (1:1000; BD Transduction Laboratories), mouse anti-Rab5 (1:1000; from Hybridoma, CL621.3), rabbit anti-Rab4 antibodies (1:1000; Abcam), and Mouse anti-actin (1:500,000; Millipore) were used for immunoblotting. Alexa-Fluor-488- or Alexa-Fluor-568-tagged goat anti-mouse- or anti-rabbit-immunoglobulin antibodies (1:200; Molecular Probes) were used as secondary antibodies for immunofluorescence, and horseradish-peroxidase-coupled goat anti-mouse- or anti-rabbit-immunoglobulin antibodies (1:5000; Sigma Immunochemicals) in combination with the enhanced chemiluminescence reaction kit (Amersham Pharmacia Biotech) were used for immunoblot analysis. For immunoprecipitation, rabbit anti-Rbpt5 (1:300; Novus Biologicals) and mouse anti-HA (1:300; hybridoma 12CA5) antibodies were used.

Acknowledgements

We particularly thank Nicole Beuret for her support and are grateful to the Biozentrum Imaging Core Facility, to Peter van der Sluijs, Marino Zerial and Elizabeth Smythe for materials, Philipp Berger, Kurt Ballmer-Hofer and Andriana Kriz for MultiLabel and Aurélien Rizk for his quantification software before publication.

Competing interests
The authors declare no competing or financial interests.

Author contributions
S.K. and M.S. designed the study. S.K. performed and analyzed most of the experiments. D.T.H. and D.P.B. contributed additional experiments. S.K. and M.S. wrote the manuscript.

Funding
This work was supported by the Swiss National Science Foundation [grant number 31003A-125423]. D.P.B. was supported by the Fellowships for Excellence PhD program of the Werner Siemens Foundation and the University of Basel.

Supplementary information
Supplementary information available online at
http://jcs.biologists.org/lookup/suppl/doi:10.1242/jcs.174664/-/DC1

References
Barr, F. A. (2013). Rab GTPases and membrane identity: causal or inconsequential? *J. Cell Biol.* **202**, 191-199.
Blümer, J., Rey, J., Dehmelt, L., Mazel, T., Wu, Y.-W., Bastiaens, P., Goody, R. S. and Itzen, A. (2013). RabGEFs are a major determinant for specific Rab membrane targeting. *J. Cell Biol.* **200**, 287-300.
Bolte, S. and Cordelières, F. P. (2006). A guided tour into subcellular colocalization analysis in light microscopy. *J. Microsc.* **224**, 213-232.
Bucci, C., Parton, R. G., Mather, I. H., Stunnenberg, H., Simons, K., Hoflack, B. and Zerial, M. (1992). The small GTPase rab5 functions as a regulatory factor in the early endocytic pathway. *Cell* **70**, 715-728.
Carpenter, A. E., Jones, T. R., Lamprecht, M. R., Clarke, C., Kang, I. H., Friman, O., Guertin, D. A., Chang, J. H., Lindquist, R. A., Moffat, J. et al. (2006). CellProfiler: image analysis software for identifying and quantifying cell phenotypes. *Genome Biol.* **7**, R100.
Christoforidis, S., McBride, H. M., Burgoyne, R. D. and Zerial, M. (1999a). The Rab5 effector EEA1 is a core component of endosome docking. *Nature* **397**, 621-625.
Christoforidis, S., Miaczynska, M., Ashman, K., Wilm, M., Zhao, L., Yip, S.-C., Waterfield, M. D., Backer, J. M. and Zerial, M. (1999b). Phosphatidylinositol-3-OH kinases are Rab5 effectors. *Nat. Cell Biol.* **1**, 249-252.
De Renzis, S., Sönnichsen, B. and Zerial, M. (2002). Divalent Rab effectors regulate the sub-compartmental organization and sorting of early endosomes. *Nat. Cell Biol.* **4**, 124-133.
Delprato, A. and Lambright, D. G. (2007). Structural basis for Rab GTPase activation by VPS9 domain exchange factors. *Nat. Struct. Mol. Biol.* **14**, 406-412.
Deneka, M., Neeft, M., Popa, I., van Oort, M., Sprong, H., Oorschot, V., Klumperman, J., Schu, P. and van der Sluijs, P. (2003). Rabaptin-5alpha/rabaptin-4 serves as a linker between rab4 and gamma(1)-adaptin in membrane recycling from endosomes. *EMBO J.* **22**, 2645-2657.
Haas, A. K., Fuchs, E., Kopajtich, R. and Barr, F. A. (2005). A GTPase-activating protein controls Rab5 function in endocytic trafficking. *Nat. Cell Biol.* **7**, 887-893.
Hirota, Y., Kuronita, T., Fujita, H. and Tanaka, Y. (2007). A role for Rab5 activity in the biogenesis of endosomal and lysosomal compartments. *Biochem. Biophys. Res. Commun.* **364**, 40-47.
Hirschmann, D. T., Kasper, C. A. and Spiess, M. (2015). Quantitative analysis of transferrin cycling by automated fluorescence microscopy. *Methods Mol. Biol.* **1270**, 365-378.
Horiuchi, H., Lippé, R., McBride, H. M., Rubino, M., Woodman, P., Stenmark, H., Rybin, V., Wilm, M., Ashman, K., Mann, M. et al. (1997). A novel Rab5 GDP/GTP exchange factor complexed to Rabaptin-5 links nucleotide exchange to effector recruitment and function. *Cell* **90**, 1149-1159.
Huotari, J. and Helenius, A. (2011). Endosome maturation. *EMBO J.* **30**, 3481-3500.
Korobko, E., Kiselev, S., Olsnes, S., Stenmark, H. and Korobko, I. (2005). The Rab5 effector Rabaptin-5 and its isoform Rabaptin-5delta differ in their ability to interact with the small GTPase Rab4. *FEBS J.* **272**, 37-46.
Korobko, E. V., Palgova, I. V., Kiselev, S. L. and Korobko, I. V. (2006). Apoptotic cleavage of rabaptin-5-like proteins and a model for rabaptin-5 inactivation in apoptosis. *Cell Cycle* **5**, 1854-1858.
Kriz, A., Schmid, K., Baumgartner, N., Ziegler, U., Berger, I., Ballmer-Hofer, K. and Berger, P. (2010). A plasmid-based multigene expression system for mammalian cells. *Nat. Commun.* **1**, 120.
Kümmel, D. and Ungermann, C. (2014). Principles of membrane tethering and fusion in endosome and lysosome biogenesis. *Curr. Opin. Cell Biol.* **29**, 61-66.
Lippé, R., Miaczynska, M., Rybin, V., Runge, A. and Zerial, M. (2001). Functional synergy between Rab5 effector Rabaptin-5 and exchange factor Rabex-5 when physically associated in a complex. *Mol. Biol. Cell* **12**, 2219-2228.
Mattera, R. and Bonifacino, J. S. (2008). Ubiquitin binding and conjugation regulate the recruitment of Rabex-5 to early endosomes. *EMBO J.* **27**, 2484-2494.
Mattera, R., Arighi, C. N., Lodge, R., Zerial, M. and Bonifacino, J. S. (2003). Divalent interaction of the GGAs with the Rabaptin-5-Rabex-5 complex. *EMBO J.* **22**, 78-88.
Mattera, R., Tsai, Y. C., Weissman, A. M. and Bonifacino, J. S. (2006). The Rab5 guanine nucleotide exchange factor Rabex-5 binds ubiquitin (Ub) and functions as a Ub ligase through an atypical Ub-interacting motif and a zinc finger domain. *J. Biol. Chem.* **281**, 6874-6883.
Mizuno-Yamasaki, E., Rivera-Molina, F. and Novick, P. (2012). GTPase networks in membrane traffic. *Annu. Rev. Biochem.* **81**, 637-659.
Nielsen, E., Christoforidis, S., Uttenweiler-Joseph, S., Miaczynska, M., Dewitte, F., Wilm, M., Hoflack, B. and Zerial, M. (2000). Rabenosyn-5, a novel Rab5 effector, is complexed with hVPS45 and recruited to endosomes through a FYVE finger domain. *J. Cell Biol.* **151**, 601-612.
Ohya, T., Miaczynska, M., Coskun, U., Lommer, B., Runge, A., Drechsel, D., Kalaidzidis, Y. and Zerial, M. (2009). Reconstitution of Rab- and SNARE-dependent membrane fusion by synthetic endosomes. *Nature* **459**, 1091-1097.
Pfeffer, S. R. (2013). Rab GTPase regulation of membrane identity. *Curr. Opin. Cell Biol.* **25**, 414-419.
Poteryaev, D., Datta, S., Ackema, K., Zerial, M. and Spang, A. (2010). Identification of the switch in early-to-late endosome transition. *Cell* **141**, 497-508.
Rink, J., Ghigo, E., Kalaidzidis, Y. and Zerial, M. (2005). Rab conversion as a mechanism of progression from early to late endosomes. *Cell* **122**, 735-749.
Rizk, A., Paul, G., Incardona, P., Bugarski, M., Mansouri, M., Niemann, A., Ziegler, U., Berger, P. and Sbalzarini, I. F. (2014). Segmentation and quantification of subcellular structures in fluorescence microscopy images using Squassh. *Nat. Protoc.* **9**, 586-596.
Stenmark, H. (2009). Rab GTPases as coordinators of vesicle traffic. *Nat. Rev. Mol. Cell Biol.* **10**, 513-525.
Stenmark, H., Parton, R. G., Steele-Mortimer, O., Lütcke, A., Gruenberg, J. and Zerial, M. (1994). Inhibition of rab5 GTPase activity stimulates membrane fusion in endocytosis. *EMBO J.* **13**, 1287-1296.
Stenmark, H., Vitale, G., Ullrich, O. and Zerial, M. (1995). Rabaptin-5 is a direct effector of the small GTPase Rab5 in endocytic membrane fusion. *Cell* **83**, 423-432.
Vitale, G., Rybin, V., Christoforidis, S., Thornqvist, P.-Ö., McCaffrey, M., Stenmark, H. and Zerial, M. (1998). Distinct Rab-binding domains mediate the interaction of Rabaptin-5 with GTP-bound Rab4 and Rab5. *EMBO J.* **17**, 1941-1951.
Wegener, C. S., Malerød, L., Pedersen, N. M., Progida, C., Bakke, O., Stenmark, H. and Brech, A. (2010). Ultrastructural characterization of giant endosomes induced by GTPase-deficient Rab5. *Histochem. Cell Biol.* **133**, 41-55.
Zerial, M. and McBride, H. (2001). Rab proteins as membrane organizers. *Nat. Rev. Mol. Cell Biol.* **2**, 107-117.
Zhu, G., Zhai, P., He, X., Wakeham, N., Rodgers, K., Li, G., Tang, J. and Zhang, X. C. (2004a). Crystal structure of human GGA1 GAT domain complexed with the GAT-binding domain of Rabaptin5. *EMBO J.* **23**, 3909-3917.
Zhu, G., Zhai, P., Liu, J., Terzyan, S., Li, G. and Zhang, X. C. (2004b). Structural basis of Rab5-Rabaptin5 interaction in endocytosis. *Nat. Struct. Mol. Biol.* **11**, 975-983.
Zhu, H., Zhu, G., Liu, J., Liang, Z., Zhang, X. C. and Li, G. (2007). Rabaptin-5-independent membrane targeting and Rab5 activation by Rabex-5 in the cell. *Mol. Biol. Cell* **18**, 4119-4128.
Zhu, H., Qian, H. and Li, G. (2010). Delayed onset of positive feedback activation of Rab5 by Rabex-5 and Rabaptin-5 in endocytosis. *PLoS ONE* **5**, e9226.